Since January 2020 Elsevier has created a COVID-19 resource centre with free information in English and Mandarin on the novel coronavirus COVID-19. The COVID-19 resource centre is hosted on Elsevier Connect, the company's public news and information website.

Journal of Building Engineering 42 (2021) 103090

Contents lists available at ScienceDirect

Journal of Building Engineering

journal homepage: www.elsevier.com/locate/jobe

Study on ventilation rates and assessment of infection risks of COVID-19 in an outpatient building

Chunying Li, Haida Tang *

School of Architecture and Urban Planning, Shenzhen University, Shenzhen, China

ARTICLE INFO

Keywords:
COVID-19
Infection risk
Ventilation rate
Wells-Riley model
Hospital

ABSTRACT

A modified Wells-Riley model combining the airborne route and close contact route was proposed to predict the infection risks of coronavirus disease 2019 (COVID-19) in main functional spaces of an outpatient building in Shenzhen, China. The personnel densities and ventilation rates in the 20 waiting rooms, outpatient hall and hospital street were on-site measured. The average fresh air volume per person and occupant area per person in the 20 waiting rooms were 77.6 m^3/h and 6.47 m^2/per, satisfied with the Chinese standard. The average waiting time of the occupants was 0.69 h. Thus, assuming the proportion of infected people in the outpatient building was 2%, the daily average infection probabilities of COVID-19 in the 20 waiting rooms were 0.19–1.88% with a reasonable setting of the quanta produced by an infector ($q = 45$ quanta/h) and the effective exposure dose of pathogen per unit close contact time ($\beta = 0.05$ h^{-1}). The design of the semi-closed hospital street with a height of 24 m improved its natural ventilation with a fresh air volume per person of 70–185 m^3/h and further dilute the viral aerosol and decreased the infection risk to a negligible level (i.e., below 0.04% with an infector proportion of 2%). The assessment method provides real-time prediction of indoor infection risk and good assist in spread control of COVID-19.

1. Introduction

1.1. Background

The outbreak of coronavirus disease 2019 (COVID-19) is causing worldwide attention. To diminish the risk of human to human transmission, governments request reducing crowd gathering and wearing masks, especially in closed spaces [1]. Scientists around the word called for attention to the airborne transmission of COVID-19 [2]. As many reports revealed the cross-infection between patients and doctors, hospital is recognized as a place with high infection risk. A retrospective analysis of 138 patients with COVID-19 by the Central South Hospital of Wuhan University showed that 41.3% of the infections might occur in hospitals [3]. Among the cases, there was an inpatient of surgical department who caused infections of more than 10 staff. Up until February 11, 2020, 3019 hospital staff were infected with COVID-19 in 422 medical institutions in China [4]. Moreover, the infection risk exists in not only respiratory department but other departments as well, such as ophthalmology and dentistry [5]. It is of great importance to optimize the hospital design and operation to control the spread of COVID-19 among occupants [6,7]. For this purpose, it is essential to develop a reliable and practical method to predict the infection risk.

Multiple models were developed to provide quantitative predictions of airborne disease infection risks, including the SI model, SIS model, SIR model and so on [8]. The Wells-Riley model allows quick assessment and has been widely used in the epidemic modeling since its development by Riley in 1978 [9]. The concept of quantum is utilized as the minimum dose of airborne pathogens (either attached to the droplets or aerosols) to cause infection in a closed space, which was firstly brought forward by Wells in 1955 [10]. In this way, the infection risk is directly related to the ventilation, exposure duration and ratio of infected people in the crowd [11,12].

During the past decades, the Wells-Riley model has been used to calculate infection risks in airliner cabins, buses, hospital wards, schools, prison inmates, nightclubs, social halls and so on [13–16]. Yan [13] used the Wells-Riley model in the evaluation of airborne disease infection risks in a Boeing 737 airliner cabin with the Lagrangian tracking process. You [14] compared the infection risks of similar airline cabin with three different ventilation systems. Qian [15] applied the Wells-Riley model in the assessment of severe acute respiratory

* Corresponding author.
E-mail address: tanghd@szu.edu.cn (H. Tang).

https://doi.org/10.1016/j.jobe.2021.103090
Received 23 March 2021; Received in revised form 2 August 2021; Accepted 5 August 2021
Available online 10 August 2021

syndrome coronavirus (SARS) infection risk in a hospital ward, with the spatial distribution of the risk taken into consideration. The inter-cube spread trend of SARS was predicted and well validated with observed data. In addition, the Wells-Riley model was also applied in the prediction of accumulated long-term airborne disease infection risk. Hella [16] estimated the annual risks of tuberculosis transmission using the Wells-Riley model for different locations. The results revealed high risk of infection in prison inmates (41.6%) and drivers in public transport (20.3%). With the advantages of flexible and universal applicability, the Wells-Riley model have been applied to assess infection risks of COVID-19 in built environment [9,17,18].

Ventilation is commonly accounted as efficient to dilute the virus-attached droplets and aerosols, and therefore to reduce the infection risks [19,20]. Many investigations applied the Wells-Riley model to testify this point. The work of Zhu [21] focused on the airborne disease spread in bus micro-environments. Numerical model combing the Wells-Riley model and CFD simulation was developed and utilized. The results demonstrated the displacement ventilation method to be the most effective in limiting the risk of airborne infection. Steady [22] assessed the transmission of tuberculosis in prison with the aid of the Wells-Riley model. Calculation results implied an air change rate of as high as 8 h^{-1} was necessary to protect the occupants from infection. The effectiveness of ventilation was also compared with other measures in control of disease spread. For example, different school interventions concerning infectious disease spread were evaluated based on Wells-Riley model by Gao [23]. With hypothetical school contact activities, the infection risks were calculated and the results demonstrated that increasing air change rate together with household isolation could be as effective as school closure.

As above-mentioned studies theoretically confirmed thorough ventilation as an efficient and economic measure to reduce the airborne disease spread, there are few experimental investigations [24]. Wu [25] carried out on-site measurement of tracer gas (SF_6) transmission between horizontal adjacent flats in residential building. The air change rates of typical Hong Kong flats were calculated based on the experimental data, and the cross-infection risks were estimated with the Wells-Riley model. Nevertheless, most of the densely populated spaces were in public buildings, and the on-site measurement with tracer gas easily causes safety concerns. Because of this issue, theoretical calculations mostly used standard personnel densities and air change rates, whereas the possibility of applying the Wells-Riley model in operating buildings was not given fully attention. Moreover, the air change rates in built environment are seldom stable, as infiltration constantly introduce indoor-outdoor air change through window slits and door gaps unpredictably. For places where people frequently enter or exit, the ventilation is enhanced on a certain level and precise calculation is almost impossible. All these issues stress the importance of field measurement when ventilation is concerned.

On the other hand, the ventilation condition in hospitals is commonly evaluated as an important measure to improve the indoor air quality, to enhance the patient recovery, to improve the physical and mental health of hospital staff. Researchers have associated inadequate indoor air ventilation with outbreaks of infection in clinical and non-clinical settings [26,27]. Stockwell [28] reviewed 36 journal articles concerning indoor micro-organism and ventilation in hospitals, and stressed the importance of mechanical ventilation as an effective infection-control strategy. Innovative ventilation systems were brought forward to improve the indoor air quality in hospitals [29]. Qian [30] and Tang [31] carried out on-site measurement of ventilation in hospital wards in Hong Kong and Shenzhen. Their results showed different outcomes: the high efficiency of natural ventilation (in Qian's research, with air change rate as high as 11.9–69.0 h^{-1}) and lack of fresh air with mechanical ventilation (in Tang's research, with air change rate of 1.1 h^{-1} on average). The sharp contrast revealed that there wasn't a superior choice between mechanical and natural ventilation. There are circumstances that these two ventilation measures need to be applied together.

In summary, it is commonly recognized that ventilation is of significant importance to infection risk of building occupants when facing the pandemic of COVID-19 [17–20]. Though infection risks of COVID-19 in hospitals are rising more and more attention, there are few literature focusing on the assessment of the reduction of infection risks with ventilation rate from field measurement. On the contrary, recommended air change rate from standards or guidelines were frequently applied in risk assessment, which cannot represent the real condition. In reality, ventilation rates are influenced by multiple factors, including the ventilation modes, location and size of the openings, heat source within the building, system operation & management and so on [32,33]. When evaluating infection risks of COVID-19, it is important to acquire the actual ventilation rate.

To fill this gap, a practical approach combining physical measurement and theoretical calculation is brought forward and utilized to predict the infection risks of COVID-19 in the present investigation. The aim is to improve the accuracy of the infection risks assessment with alternative source of data (ventilation rate and occupant behavior) instead of bare assumptions. The ventilation rates were obtained through consistent measurement of the tracer gas (CO_2 from breathing is used in the present stage) [34]. Currently, the occupant number and dwell time was acquired directly from on-site observation. To our best knowledge, it is novel to introduce occupant behavior to the prediction of airborne disease transmission in built environment. Based on these information, the temporal and spatial infection risks were calculated with a modified Wells-Riley model combining the airborne route and close contact route. In conclusion, the present study provides a novel and realistic approach for the infection risk of COVID-19 in closed spaces, with the expense of real-time monitoring on limited parameters.

2. Building information

The physical measurement and on-site observation in an outpatient building were completed in July 2018. Back then, there was no airborne disease pandemic alert and the hospital was in normal operation. The hospital was located in Shenzhen, with hot summer and warm winter climate. The outpatient building was 211 m long, 115 m wide and 24 m high (4 stories). There were in total 35 departments separated on the 4 stories, providing comprehensive medical service. Fig. 1 shows the floor plans of the building, and Fig. 2 shows the inner view of the main functional spaces.

As shown in Fig. 1(a), the hospital street lied along the central axis of the building, connecting the outpatient departments on the southern side and medical technology departments on the northern side. The hospital street was 112 m long, 28 m wide and 24 m high. There was long ceiling opening above the hospital street (as illustrated in Fig. 2(b)), which constantly introduced air change between the hospital street and outdoor. Moreover, there were 7 entrances to the hospital street on the 1st floor, which were in direct connection with the ambient environment, as demonstrated in Fig. 1(a) (with signs of A-G). There were air-conditioning systems supplying conditioned air to the waiting rooms and the outpatient hall. The air distribution of the waiting rooms was through supply and return ceiling diffuser. The air supply nozzles (4 m from the floor) on the wall supplied conditioned air to the outpatient hall. The supplied air was well-mixed in the occupied zone before recirculated through the air outlet on the other side wall.

Most of the patients entered the outpatient building through the outpatient hall in the western side (Fig. 2(a)). The outpatient hall was 12–18 m long, 115 m wide and 18 m high. The patients firstly picked up registration cards in the registration charge (the orange color block in Fig. 1(a), i.e., the north-side of the outpatient hall) and went to the outpatient departments through the hospital street (Fig. 2(b)). There was one waiting room in each department (Fig. 2(c)), with automatic doors open directly to the hospital street. The areas of the investigated waiting rooms in the outpatient building were listed in Table 1. The

(a) 1st floor

(b) 2nd floor

(c) 3rd floor

(d) 4th floor

Fig. 1. Floor plans of the outpatient building.

(a) Outpatient hall (b) Hospital street (c) Waiting room

Fig. 2. Inner view of functional spaces of the outpatient building.

Table 1
Areas of the waiting rooms in various departments.

1F		2F		3F		4F	
Department	area (m^2)	Department	area (m^2)	department	area (m^2)	department	area (m^2)
Ultrasound	106	Respiratory	136	urology	136	dermatology	106
Radiology	228	Nephrology	106	obstetric	177	ophthalmology	177
Pediatrics	370	Orthopedics	177	gynecology	218	E.N.T.	202
internal medicine	191	ECG	218	anesthesiology	106	dental	172
outpatient hall	1725	neurosurgery	176	hepatology	119		
hospital street	3136	gastroenterology	106	blood collection	188		

areas of the waiting rooms varied in the range of 106–370 m^2. The heights of the waiting rooms were 4.8 m for the 1st floor and 3.7 m for the 2nd - 4th floors. The waiting rooms were equipped with central air-conditioning system with mechanical fresh air supply. The air-conditioning system was on operation during working hours throughout the year to maintain a micro-positive pressure, whereas the hospital street was not air-conditioned. For each patient, his/her waiting time is depended on the number of doctors and patients. After consulting the doctor, the patients either went to the medical technology departments for medical test or to pick up medicine at the pharmacy (the purple color block in Fig. 1(a), i.e. south-side of the outpatient hall), and then left.

3. Methodology

3.1. Physical measurement and on-site observation

Ventilation in the functional spaces of the outpatient hospital were investigated by physical measurement. CO_2 concentration sensor of Telaire 7001 model was used to measure indoor CO_2 concentration, with measurement range of 0–10000 ppm and accuracy of ±50 ppm. The measured CO_2 concentration reflected its absolute value. As for the outdoor CO_2 concentration, it was monitored with a meteorological station on the roof of the building. For all measuring points, Telaire 7001 instruments were located 1.2 m height from the floor. There were 44 measuring points in the hospital street with an 8 m × 7 m grid, and 36 measuring points in the outpatient hall with a 9 m × 3 m grid. For every waiting room, 5 measuring points were evenly distributed - 1 point in the room center and 4 points along the diagonal line.

Both indoor and outdoor CO_2 concentrations were utilized to calculate the ventilation rates of the functional spaces. This method is popular to ascertain the ventilation condition [34–36]. It should be noted that the calculation is based on the assumption of well-mixed air in the space. Considering the outpatient building under investigation is a large-scale complex building and there are over 10,000 visits daily (including the patients, companions and hospital staff), CO_2 from occupants breathing is the safest tracer gas for ventilation testing. Therefore, the ventilation rate is calculated as follows:

$$Q = \frac{kn_w}{C_i - C_o} \tag{1}$$

where, C_i and C_o are the indoor and outdoor CO_2 concentration, ppm; k is the CO_2 emission per person, which is influenced by the factors including gender, activity and age, m^3/h, which is calculated with Eq. (2) [37].

$$k = \varepsilon \cdot RQ \frac{0.00056028 H^{0.725} W^{0.425} M}{0.23RQ + 0.77} \tag{2}$$

where, ϵ is a recommended revised factor for the CO_2 emission calculation, and is 1.0 for male and 0.75 for female occupants, -; RQ is the respiratory quotient (molar ratio of CO_2 exhaled to O_2 inhaled), -; H and W are the height (m) and weight (kg) of a typical Chinese human; M is the metabolic rate of people sitting in peace, which is assumed to be 58.5 W/m^2 in the calculation. Considering the observed equal proportion of male and female occupants in the outpatient building, the average value of $k = 0.018$ m^3/h is used in the calculation. According to the survey data, the relative deviation of the height (H), weight (W) and metabolic rate (M) were approximately 10%. The relative deviation of the occupant number in an hour was approximately 15%. The CO_2 concentration difference between the indoor and outdoor ranged 100–580 ppm, with an average value of 258 ppm. As a result, the relative deviation of the measured CO_2 concentration was 19%. The relative deviation of the ventilation rates in each enclosed space was 28% calculated through the error transfer formula.

The number of occupants including patients, companions, hospital staff in the functional spaces were counted hourly through on-site observation. The occupant area per person (ω) is the ratio of the room area to the occupant number. The exposure duration of patients (t) is calculated based on the on-site observation and Eq. (3).

$$t = \frac{n_p t_c}{n_d} = \frac{n_w \sigma t_c}{n_d} \tag{3}$$

where, n_w, n_p and n_d are respectively the numbers of occupants, patients

and doctors on duty in the specific department, person; σ is the ratio of patients to total occupants, -; and t_c is the average duration of the patient consulting with the doctor, h. The calculation of the exposure duration (t) (Eq. (3)) is based on the assumption of first-come-first-served principle. When a certain patient enters the waiting room, there are already n_p patients waiting. This patient need to wait until the n_p patients left the waiting room to consult the n_d doctors on duty.

3.2. Model of airborne disease infection risk

The Wells-Riley model is based on the quantal infection and widely applied in the evaluation of airborne disease infection risks, including the global-sweeping COVID-19 [9].

$$P^a = 1 - \exp\left(-\frac{I_a q p t}{Q}\right) = 1 - \exp\left(-\frac{q p \phi t}{q_m}\right) \tag{4}$$

where, P^a is the probability of infection of COVID-19 through airborne transmission, -; I_a is the number of the infectors in the closed space, -; q is the quanta produced by an infector, quanta/h; p is the pulmonary ventilation rate of each occupant per hour, 0.48 m^3/h; and t is the exposure duration, h; Q is the ventilation rate of the space, m^3/h; q_m is the fresh air volume per person, m^3/h; ϕ is the proportion of infected people in the crowd, which is calculated by subdividing the total occupants with total infectors number, -. As the values of q and q_m are directly related to the viral concentration in certain space, $\frac{q}{q_m}$ represent the quantitative effect of viral aerosol dilution by fresh air. The value of $\frac{q}{q_m}$ can be a good index of dilution ratio. Consequently, higher level of $\frac{q}{q_m}$ could be a hint of relatively higher infection risk level.

Experiments have demonstrated the breath emission of SARS-CoV-2 from COVID-19 patients [38]. Investigations also confirmed the SARS-CoV-2 remaining viable in aerosols for multiple hours [39]. Evidence suggests the airborne transmission and close contact transmission should both be taken into consideration for spread control of COVID-19. Therefore, the Wells-Riley model was modified in the present study, which combined the exponential dose-response model (Eq. (5)) for prediction of the infection probability of COVID-19 through the route of close contact [40].

$$P^c = 1 - \exp(-\beta I_c t) = 1 - \exp\left(-\frac{4\pi\beta\phi t}{\omega}\right) \tag{5}$$

where, P^c is the probability of COVID-19 infection through close contact transmission, -; β is the effective exposure dose of pathogen per unit close contact time, h^{-1}; I_c is the number of close contacts with infectors in a closed space. ω is the occupant area per person, m^2/per. It is noted that spread of COVID-19 through close contact route is limited in the distance of 2 m. As a result, I_c is the number of infectors within the imaginary circle with a radius of 2 m in the closed space. In this study, the occupants are assumed distributing uniformly in every room and the infectors are assumed to be uniformly mixed in the crowd. The value of β is approximately equal to the infection probability through close contact route for a susceptible person keeping a distance under 2 m with an infector for an hour.

Considering that both airborne transmission and close contact transmission participate in the infection process, the probability of infection was calculated with a modified Wells-Riley model which assumed independent transmissions through airborne and close contact routes [41].

$$P = 1 - (1 - P^a)(1 - P^c) = 1 - \exp\left(-\left(\frac{qp}{q_m} + \frac{4\pi\beta}{\omega}\right)\phi t\right) \tag{6}$$

Considering the filtration effect of the medical surgical mask, the modified Wells-Riley model is expressed as follows:

$$P = 1 - \exp\left(-\left(\frac{qp}{q_m} + \frac{4\pi\beta}{\omega}\right)(1 - \eta_I)(1 - \eta_s)\phi t\right) \tag{7}$$

where η_I is the exhalation filtration efficiency, -; η_s is the respiratory filtration efficiency, -. In this study, the exhalation (η_I) and respiratory filtration efficiency (η_s) of the medical surgical masks are assumed to be 50%. The filtration efficiency of ordinary medical surgical masks on virus-laden aerosols is about 60% [42], which is set as 50% considering the influence of air leakage [43].

The calculation of air change rate was based on the assumption of steady indoor CO_2 concentration. Whereas the occupant numbers in functional spaces were not fixed, resulting in unstable CO_2 concentration, which inevitably brought error into the results. The error was examined together with the measurement error of both indoor and outdoor CO_2 concentrations (Eq. (8)).

$$\frac{\Delta Q}{Q} = \sqrt{\left(\frac{\partial Q}{\partial n_w}\right)^2 \Delta n_w^2 + \left(\frac{\partial Q}{\partial C_i}\right)^2 \Delta C_i^2 + \left(\frac{\partial Q}{\partial C_o}\right)^2 \Delta C_o^2} \tag{8}$$

4. On-site measurement results

4.1. Ventilation effect

There were in total 22 functional spaces covered in the measurement, including the outpatient hall, the hospital street and 20 waiting rooms of outpatient/medical technology departments distributed on the 4 stories. The measurement was carried out from 9:00–12:00 and 14:00–17:00 on a Tuesday, i.e., July 17, 2018. In Shenzhen, the cooling season is as long as 6 months (from May to October). July is basically in the middle of the cooling season, and the natural ventilation during July can be representative for the cooling-dominant climate. In China, the hospitals are usually busy on Mondays, due to the patients piled up on weekends. As a result, the survey was carried out on Tuesday and the patients flow can better reflect occupant behavior in the outpatient building.

Fig. 3 presents the hourly indoor CO_2 concentrations in 22 functional spaces, and the values were instantaneous values. The readings were recorded after 3 min at each measuring point to make sure the readings accurately reflect the practical condition, and the fluctuation of indoor CO_2 concentrations were not obvious.

The average indoor CO_2 concentrations in 22 functional spaces during the weekday was 699 ppm. In the waiting rooms, the CO_2 concentrations increased in the morning, along with the arriving of patients and their companions. The CO_2 concentrations then dropped dramatically at noon because of the lunch break. In the afternoon, the CO_2 concentrations increased again, and then dropped as patients left the hospital. The recorded highest CO_2 concentration was 1120 ppm, at 11:00 in the waiting room of the ultrasound department, and this value exceeded the Chinese National Standard of Green Hospital Buildings (GB/T 51153-2015) [44] and Hygienic Standard for Hospital Waiting Room (GB 9671-1996) [45]. In both standards, the upper limit of indoor CO_2 concentration in waiting rooms was 1000 ppm. Similar phenomena occurred in the waiting room of the ultrasound department (at 12:00), anesthesiology department (at 15:00–16:00) and obstetric department (at 10:00). On the other hand, lower CO_2 concentration was recorded in the outpatient hall and the hospital street, in the range of 515–716 ppm. In conclusion, the indoor CO_2 concentrations in the 22 functional spaces fulfills both of the national standards for most of the time. For the waiting rooms with higher occupant density and higher level of indoor CO_2 concentrations larger volume of fresh air supply or occupants density control should be applied. This also strengthened the importance of online indoor CO_2 concentration monitoring for crowded places.

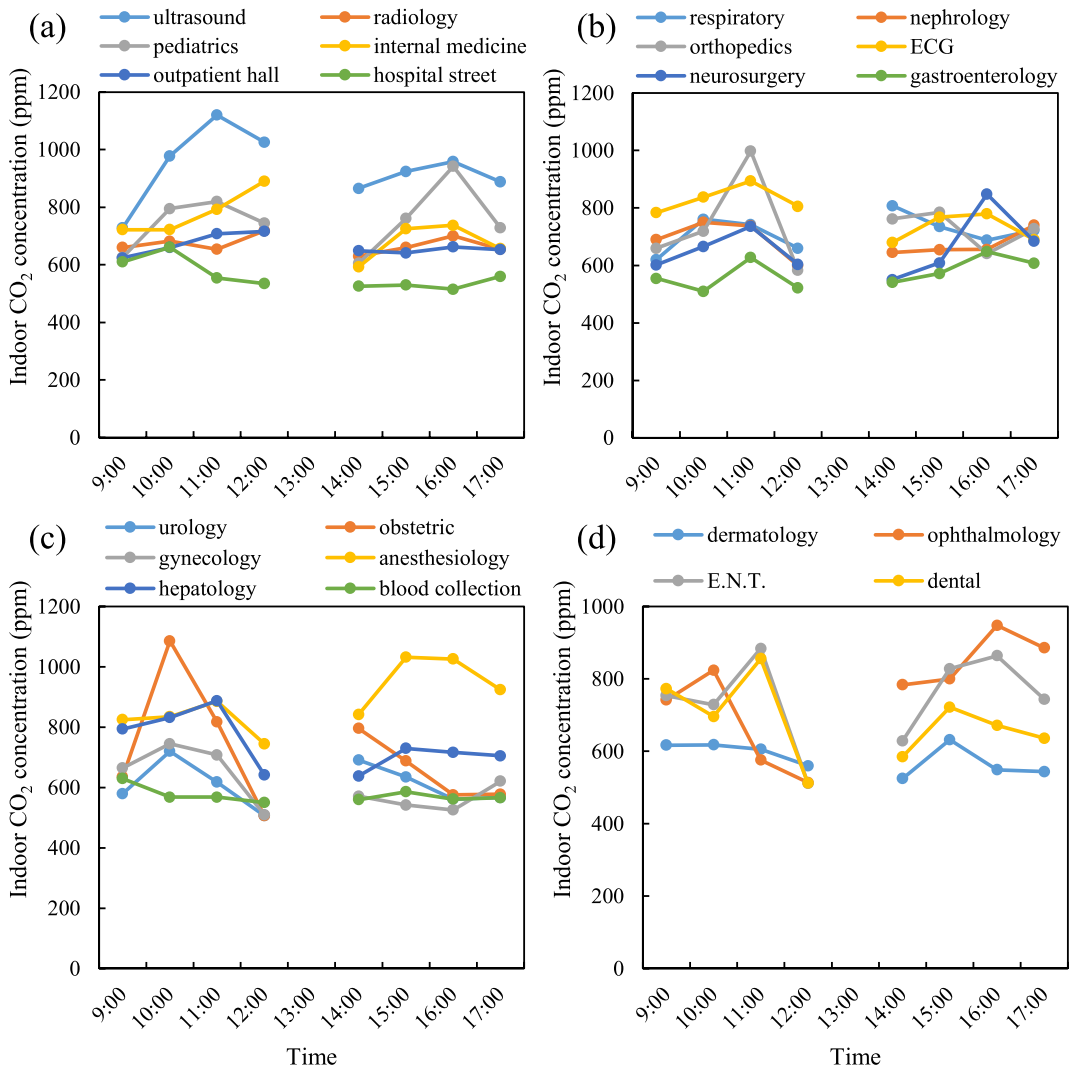

Fig. 3. Temporal variation of indoor CO2 concentration in the 22 functional spaces of the outpatient building: (a) 1st floor; (b) 2nd floor; (c) 3rd floor; and (d) 4th floor.

4.2. Occupant area per person and waiting time

For hospitals with a high level of infection risk, the occupant area per person and waiting time in closed spaces are significant factors on the infection risk of COVID-19. The occupant area per person within the above-mentioned 22 spaces were counted every hour, and the results are illustrated in Fig. 4.

Overall speaking, the average occupant area of 7.4 m^2 per person was observed for the 20 waiting rooms throughout this weekday. As for the outpatient hall and hospital street, the average occupant area of 12.7 m^2 per person was recorded. The minimum value of the occupant area per person mostly occurred at 10:00–11:00, which were quite similar with the CO_2 concentration. Different from the waiting rooms, the outpatient hall was still occupied by 220 persons at noon time, which explained the high level of CO_2 concentration in Fig. 3(a).

According to the National Code for Design of General Hospital (GB 51039-2014), the minimum waiting area of pediatrics department was 1.5 m^2 per sick child. This standard was fulfilled with the lowest occupation area of 4.5 m^2 per person (including both sick child and their companions) when this waiting room was the most crowded at 15:00. The ultrasound and anesthesiology departments with occupant areas per person of 2.6 m^2/per and 3.1 m^2/per are the most crowded among all the waiting rooms. The worst condition occurred in the ultrasound department at 11:00, and the occupant area of 1.4 m^2 per person was observed. Compared with observed data from other investigations, the condition was considered to be satisfactory. Wang [46] carried out field observation in a typical general hospital in Shanghai and reported the population density in the waiting rooms as 0.75 m^2/per during 7:30–9:30 and 1.33 m^2/per during 9:30–11:30. Ratio of patients to total occupants is also important data to predict the waiting time, i.e. the exposure duration in the waiting rooms and registration charge. According to the results of a quick questionnaire, there were 90% patients arriving the hospital with appointment in advance and 60.7% of the patients visiting the hospital with a companion.

According to Eq. (1), the ventilation rates of the waiting rooms of the different departments were calculated by the indoor and outdoor CO_2 concentration difference and the occupant number. The outdoor CO_2 concentration during the field study was in the range of 410–425 ppm and the average value of 417.5 ppm is used in the calculation. The temporal variation of the fresh air volume per person was calculated as shown in Fig. 5(a). The fresh air volume per person varied among different waiting rooms. The total average value was 77.6 m^3/h. From the aspects of both hygiene and occupant comfort, fresh air volume per person over 40 m^3/h is stipulated in the Chinese National Code for Design of General Hospital (GB 51039-2014) [47]. In Fig. 5(a), the average fresh air volume per person exceeded 40 m^3/h for the majority of the waiting rooms, i.e. the national code is fulfilled for these functional spaces. Meanwhile, the average fresh air volume per person in the

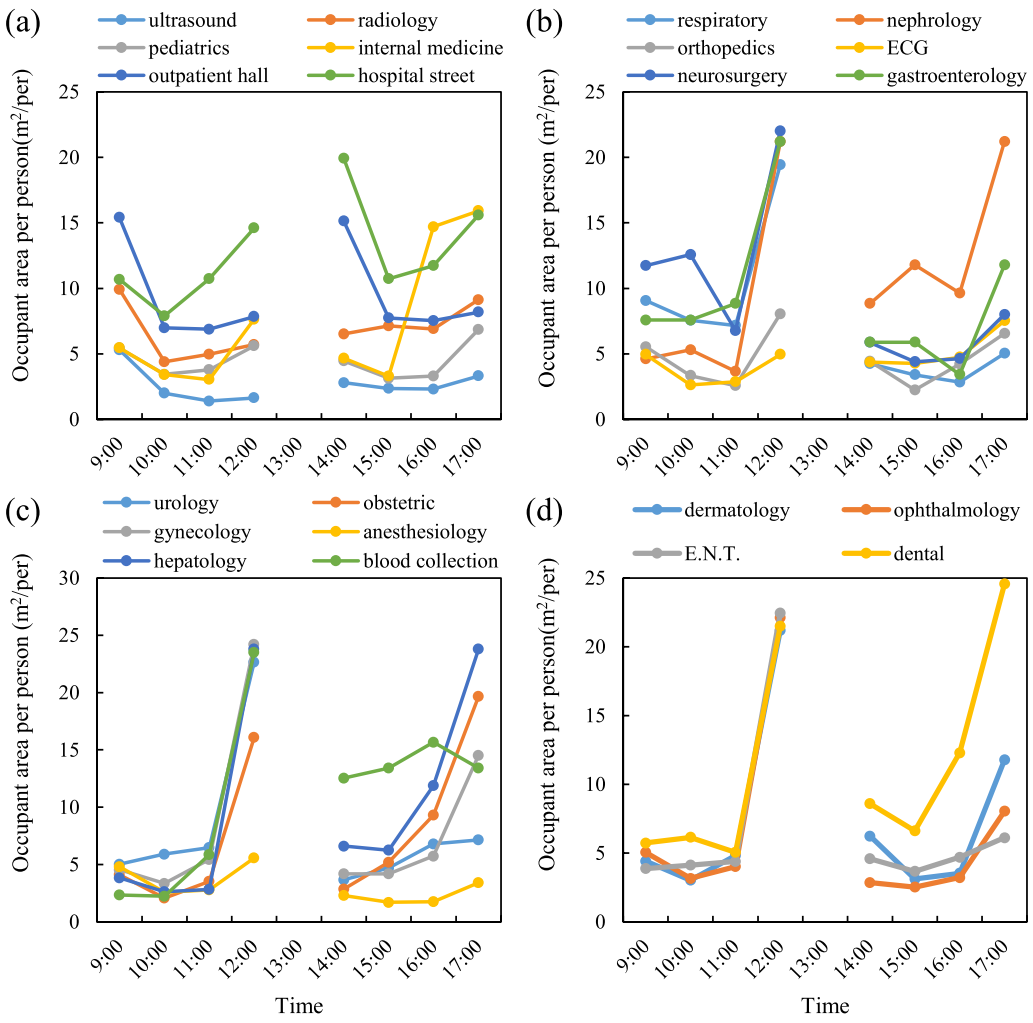

Fig. 4. Temporal variation of the occupant area per person in the 22 functional spaces of the outpatient building: (a) 1st floor; (b) 2nd floor; (c) 3rd floor; and (d) 4th floor.

waiting rooms of the ultrasound and anesthesiology departments are 36.6 m^3/h and 39.7 m^3/h, respectively. That is to say, the fresh air volumes in these two waiting rooms are slightly lower (8.5% and 0.75% less) than the standard recommendation.

The waiting time of the patients in different departments was shown in Fig. 5(b). The average waiting time in the outpatient building ranged 0.2–1.0 h with a total average value of 0.69 h.

As mentioned in Part 3.2, the unstable CO_2 concentration inevitably brought error into the results. The error was examined with Eq. (8). For the 22 functional spaces, the relative error was in the range of 8.8%–20.8%, with average value of 13.5%.

5. Assessment of infection risks of COVID-19

5.1. Infection risks with an infector proportion of 2%

The infection probability of COVID-19 for the patients and companions in the outpatient building could be calculated with Eq. (6) according to the on-site measured fresh air volume per person, occupant area per person and exposure duration. The parameters to be determined in Eq. (6) are the infector proportion in the crowd (ϕ), quanta generation rate by an infector (q) and the effective exposure dose of pathogen per unit close contact time (β). Compared with the community, a higher proportion of infected people was analyzed in the hospital. Thus, four scenarios relating to the proportion of infected people in the crowd (i.e., 2%, 5%, 10% and 15%) are applied in the present investigation. The quanta value of COVID-19 is demonstrated to diverse among asymptomatic and symptomatic subjects and individuals with different activities. In the work of Dai [9], the q value of COVID-19 is deduced to be in the range of 14–48 quanta/h according to reverse calculation based on existing epidemic cases. Meanwhile, the recommended value is in a wide range of 0.32–240 quanta/h for infector with light activity and speaking in Ref. [48].

In 1st scenario, infection risk of COVID-19 in the 20 waiting rooms was calculated with a reasonable parameter setting of $q = 45$ quanta/h, $\beta = 0.05$ h^{-1} and an infector proportion of 2%, as shown in Fig. 6. The value of β is deduced from the definition of q and statistic results in Ref. [49]. The definition of Quanta (q) was illustrated in Ref. [10], that if a person inhales one quanta of virus, the probability that they will be infected is 63%. As for the close contact, the definition of β is the effective exposure dose of pathogen per unit close contact time. Based on the statistics in Ref. [49], the infection rate was 1.8%, 2.2%, 2.9% and 4.2% for 0–17, 18–44, 45–59, and 60 or above age-groups, the average infection rate is deduced to be 2.8% after close contact with patients. Here, the assumption is that close contact of 0.5 h is long enough for COVID-19 transmission between infector and susceptible close to each other. On the condition of a close contact between one susceptible and one infector, according to Eq. (5), the equivalent β value ranged 0.03 h^{-1} to 0.09 h^{-1}, with a mean value of approximately 0.05 h^{-1}. In the assessment of the infection risks, none of the occupants in the outpatient building wore a medical surgical mask in order to better reflect the situation of the early stage of the COVID-19 pandemic.

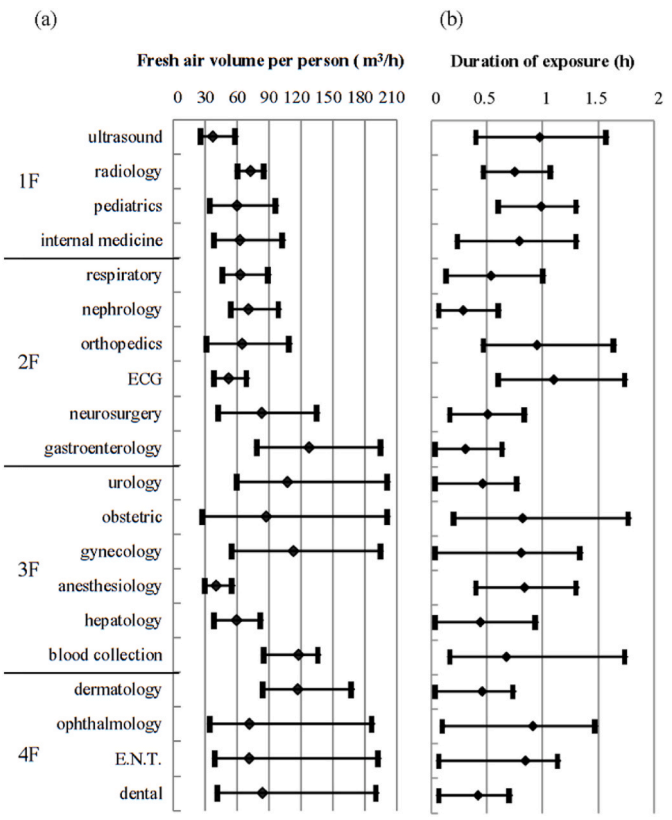

Fig. 5. Fresh air volume per person (a) and exposure duration (b) in the waiting rooms of the 20 departments.

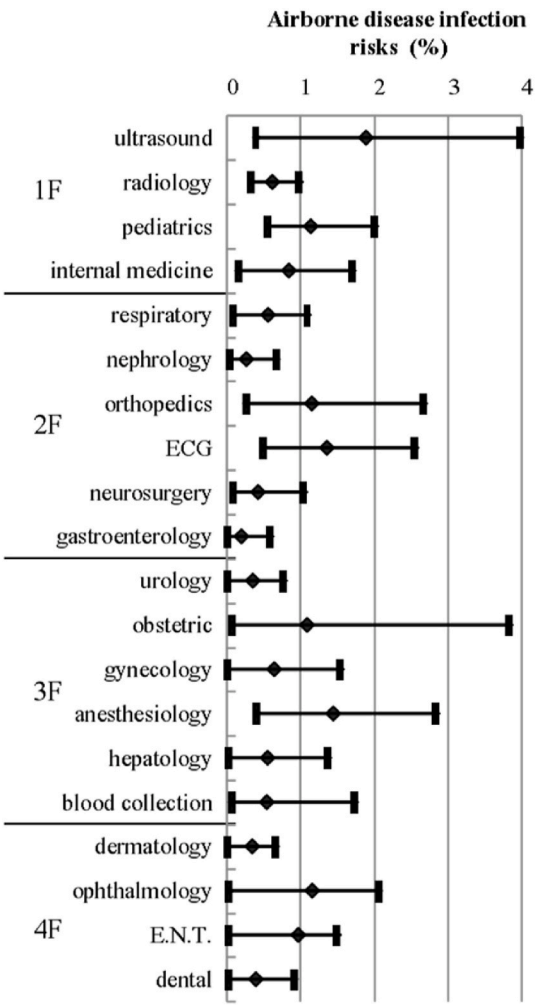

Fig. 6. Infection risks of COVID-19 in the 20 waiting rooms with a setting of q = 45 quanta/h and $\beta = 0.05\ h^{-1}$ and an infector proportion of 2%.

In Fig. 6 The infection risks of COVID-19 in the 20 waiting rooms ranged 0.19–2.63%. The highest infection risks occurred in the waiting rooms of ultrasound and anesthesiology departments. The daily average infection probability in the ultrasound and anesthesiology departments were 1.88% and 1.44%, respectively. During the investigated weekday, the average infection risks in the 20 waiting rooms were in the range of 0.19–1.88%, with the lowest risk level in the gastroenterology department and the highest risk level in the ultrasound department. The total average value of the infection risk in the 20 waiting rooms was 0.79% with an infector proportion of 2%. If one susceptible visited the ultrasound department at 10:00–12:00 or 15:00–16:00 with the highest occupant number and the lowest fresh air volume per person, the infection probability can reach up to 4%.

Almost every occupant in the hospital passes by the occupant hall and hospital street, and most likely more than once during single visit to the hospital. As shown in Fig. 7(a), the calculated fresh air volumes per person were 60–90 m^3/h in the outpatient hall and 70–185 m^3/h in the hospital street, which fulfilled the Chinese standard. The ventilation rate of the outpatient hall was close to the investigated waiting rooms. The ventilation rate in the hospital street was approximately 2 times larger than the waiting rooms. Fig. 7(b) shows the infection risks of COVID-19 with an infector proportion of 2%. For the outpatient hall, the exposure time, i.e., the waiting time for registration (or fetching medicine) was calculated with the number of occupants, the ratio of patients to the total occupants, the number of manual registration counts (or number of pharmacy counts) and the average duration of registration (or fetching medicine). According to field observation, the registration at the counter usually took around 2 min/person and the medicine fetching took around 1 min/person. Meanwhile, the registration machine also took around 2 min/person for the patients who had already made an appointment in advance. The registration machines were sufficiently equipped and there was no need to wait for using the machines. Considering the multiple functions of the hospital street, 2 sets of exposure duration (i.e., 2 min and 10 min) were applied in the assessment, which corresponded to the activities of walking pass-by and having a rest, respectively.

The infection risk of COVID-19 in the outpatient hall was less than 0.3%, and the highest risk occurred in the outpatient hall at 11:00–12:00. The infection risks were slightly higher for patients waiting at the registration counter or pharmacy, due to the longer exposure time compared with the patients using registration machines. Because of the large occupant area per person and shorter waiting time in the outpatient hall, the infection risk in the outpatient hall was just approximately eighth of that in the waiting rooms. The infection risks in the hospital street remained 0.008% for the occupants walking pass-by whose exposure duration was assumed to be 2 min and slightly increased to 0.04% for occupants having a rest, whose exposure duration was assumed to be 10 min. The results implied a low level of infection risk of COVID-19 and a relatively safe environment in the main traffic space of the outpatient building.

5.2. Sensitivity analysis

For sensitivity analysis, airborne quantum generation rates (q) of 15, 30, 45, 60, 75, 90, 105 and 120 quanta/h and the effective exposure dose of pathogen per unit close contact time (β) of 0.01, 0.02, 0.05 and 0.10 h^{-1} were applied. The range of airborne quantum generation rates (q) is set to be 15–105 h^{-1}, with the recommended values in Refs. [9,48] taken into consideration. As for the range of effective exposure dose of

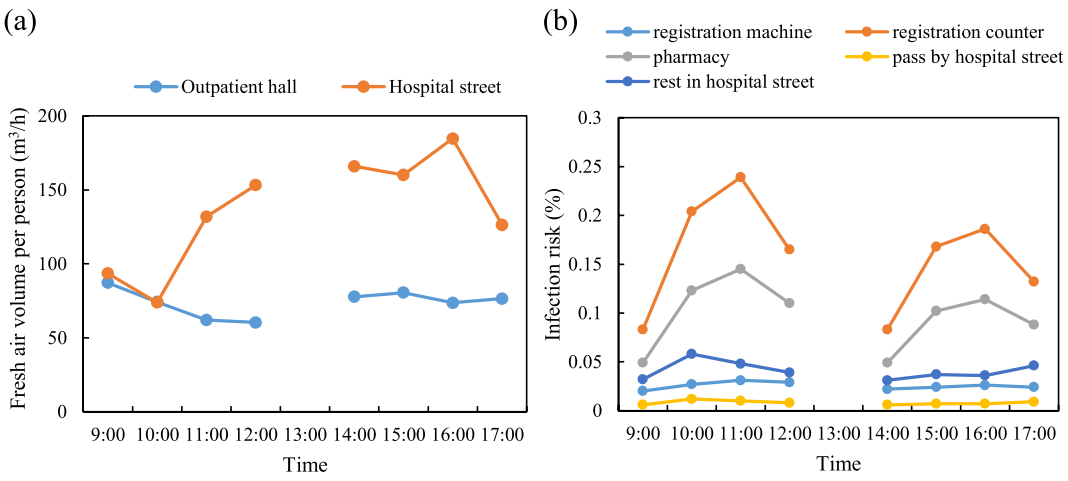

Fig. 7. Fresh air volumes per person (a) and infection risks of COVID-19 (b) in the outpatient hall and hospital street with a setting of q = 45 quanta/h and β = 0.05 h-1 and an infector proportion of 2%.

pathogen per unit close contact time (β), β is set to be 0.01–0.1 h^{-1} for sensitivity analysis. Different infector proportions (i.e., 2%, 5%, 10%, and 15%) were also taken into consideration. As the infection risk varied with time, the daily average infection risk in the 20 waiting rooms was utilized as a benchmark in the sensitivity analysis. The infection risks of the waiting rooms with different parameters setting are shown in Fig. 8. Fig. 8 shows that the infection risks increased linearly with the rising q and β.

When the proportion of the infected people was 2% (see Fig. 8(a)), the highest daily average infection risk of 1.93% was observed with the setting of $q = 120$ quanta/h and $\beta = 0.10$ h^{-1}. As the number of the total visitors to the 20 waiting rooms during the investigated workday exceeded 5000, this infection risk was quite high. During the pandemic of COVID-19, the infector proportion in the outpatient building could be higher, e.g., 5–15%. As shown in Fig. 8(b)–(d), the daily average infection risk increased approximately linearly with the infector

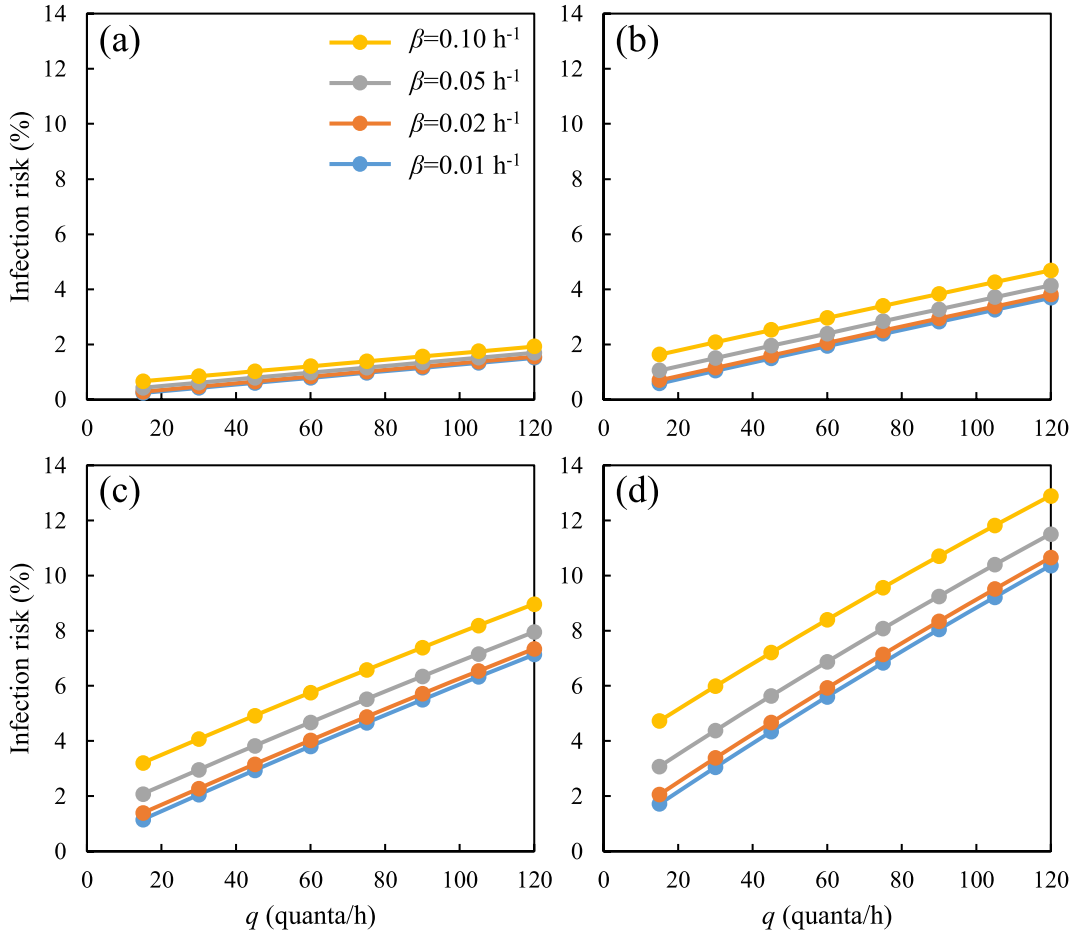

Fig. 8. Average infection risks during the working hours in the 20 waiting rooms with various infector proportions: (a) with an infector proportion of 2%; (b) with an infector proportion of 5%; (c) with an infector proportion of 10%; and (d) with an infector proportion of 15%.

proportion in the outpatient building. With a setting of $q = 45$ quanta/h and $\beta = 0.05$ h^{-1}, the daily average infection risks of the 20 waiting rooms for an infector proportion of 5%, 10% and 15% are 1.95%, 3.83%, and 5.64%, respectively. The reduction of the infection risks by wearing medical surgical masks can be estimated by Eq. (7). When each occupant in the waiting rooms wears a medical surgical mask, the daily average infection risk for an infector proportion of 5%, 10% and 15% can decrease to 0.49%, 0.97%, and 1.44%, with a setting of $q = 45$ quanta/h and $\beta = 0.05$ h^{-1}. The measure of wearing medical surgical masks decreases the infection risk by approximately 75%. In summary, the average infection risks during the working hours in the 20 waiting rooms were found to be in linear relationship with the quanta value (representing the viral release rate). Furthermore, according to the Taylor expansion formula, when the inhaled virus dose is small, the exponential form of the dose-response model for the infection risk (i.e., Eq. (7)) could be approximate to the linear form, namely, $P = \left(\frac{qp}{q_m} + \frac{4\pi\beta}{\omega}\right)(1-\eta_I)(1-\eta_s)\phi t$. As a result, when the inhaled virus dose is small, the infection risk is directly proportional to the infector proportion. Nevertheless, when the infector proportion is high, e.g., 15%, the relative deviation of the infection risk calculated with exponential formula with the linear formula is 7%. The linear relationship between infection risk and infector proportion is appropriate to the condition with a small infector proportion.

6. Discussion

6.1. Infection risks in the outpatient building

The infection probability of COVID-19 in the hospital street with a reasonable setting of $q = 45$ quanta/h, $\beta = 0.05$ h^{-1} and an infector proportion of 2% was quite low, i.e., less than 0.06%. Compared with conventional hospitals, the most extraordinary feature of this outpatient building is the semi-closed hospital street. To obtain a better understanding of the ventilation condition, air flow rates at 7 entrances of the hospital street (as illustrated in Fig. 1(a)) were measured on July 12–14, 2018 by anemometer. The flow rates were calculated as the product of average instantaneous air flow velocities (anemometer readings) and area of the entrances. For each entrance, 12 measuring points (4 × 3 in height and horizontal directions) were evenly distributed and 3 readings were recorded at each point.

As shown in Table 2, the air flow direction through the entrances depended on the weather condition. The natural ventilation rates on July 12–14, 2018, were 111500 m^3/h, 71700 m^3/h, and 57300 m^3/h, which provided sufficient fresh air to dilute the viral aerosol. The natural ventilation was enhanced by the stack effect within the semi-closed hospital street with a height of 24 m. The design of the semi-closed hospital street provides good assist in COVID-19 spread control.

On the other hand, the condition in the waiting rooms, where patients and their companions stay for a relatively longer period, is not optimistic. In Part 5.1, the infection risk of COVID-19 in the 20 waiting rooms was calculated with parameter setting of $q = 45$ quanta/h, $\beta = 0.05$ h^{-1} and an infector proportion of 2%. As a result, the average infection risks in the 20 waiting rooms were in the range of 0.19–1.88% (averaged at 0.79%), with average waiting time of 41.4 min during the investigated weekday. The total patient flow in the waiting rooms is deduced from the occupant number and average waiting time obtained from on-site survey. There should be over 8000 occupants stayed in the 20 waiting rooms throughout a typical weekday. Therefore, the newly infected occupants are then deduced to be 63 within the 20 waiting rooms. Accordingly, precautions should be carried out to reduce the infection risks and control the pandemic. The fresh air supplement should be enhanced in the waiting rooms, so that viral aerosols can be effectively diluted. It is also promising to filter the viral aerosols with air cleaners, as suggested in Ref. [50] for a gym. Meanwhile, the exposure time is an important factor to the infection risk (as in Eq. (7)). Accordingly, the overall infection probability should be lower if part of the patients wait in the hospital street and reduce their exposure duration in the waiting rooms.

By comparison, the calculated average infection risks of 0.79% with average waiting time of 41.4 min is much higher than that of a natural ventilated seafood market in the work of Zhang [51]. In Ref. [51], the customers' infection risk of SARS-CoV-2 was 0.00223% (median value) with exposure duration of 1 h. The main reason for such large discrepancy is the setting of only 1 infector in Ref. [51] and 2% infectors in the present study. Meanwhile, the calculated infection risk of patients and medical staff in a hospital room can be controlled to be no higher than 0.1% with exposure duration of 39 min and air change rate of 3.0 h^{-1} in the study of Buonanno [52]. It should be noted that the infector of [52] was set to be resting and oral breathing, with median quanta value of 0.37 quanta/h. This quanta value is much lower than the setting of present study (45 quanta/h), which could caused the large discrepancy of infection risks. This comparison emphasizes the importance of further study on virological properties of SARS-CoV-2.

The present approach is capable to assess the temporal and spatial infection risks of COVID-19 in a multi-function building. The combination of on-site measured ventilation rate and occupant behavior favors the accuracy of assessment. It is both realistic and meaningful to further apply the present approach to other types of public buildings, such as schools, shopping malls and so on. In this way, the infection risks of airborne transmission diseases (not limited to COVID-19) can be monitored and predicted more efficiently, with the expense of real-time monitoring on limited parameters.

6.2. Limitations

In this study, a modified Wells-Riley model for both airborne route and close contact route was proposed to predict the infection probability of COVID-19 in an outpatient building. The ventilation rate, occupant area per person, and exposure duration in each waiting rooms of the outpatient building were on-site measured in July 2018. This makes the assessment of the infection risks in the outpatient building better reflect the hospital infection spread condition in the early stage of COVID-19 pandemic. However, there are limitations in the present investigation

Table 2
Air flow rates at entrances of the hospital street.

		July 12 (Sunny)		July 13 (Rainy)		July 14 (Cloudy)	
Location	Floor	Flow rate (m^3/h)	Direction	Flow rate (m^3/h)	Direction	Flow rate (m^3/h)	Direction
A	1F	32162	outward	9949	outward	19949	outward
B	1F	15418	inward	6448	inward	20372	inward
C	1F	15997	inward	8584	inward	16667	outward
D	1F	8777	outward	18365	inward	14028	inward
E	1F	37283	outward	17966	inward	34211	inward
F	1F	44381	outward	15266	inward	47329	outward
G	1F	20261	outward	15041	inward	41918	outward

Note: inward represents air flow into the hospital and outward represents air flow outside of the hospital street.

by the unclear nature of COVID-19 up until now. Firstly, the quantum generation rates of both airborne route and close contact route are still not confirmed for COVID-19 and also affected by the stage of the infectious disease. Another problem lies in the fact that the occupants are distributed unevenly in the waiting rooms of the outpatient building. Whereas in the assessment they are assumed to be distributed evenly for simplicity and the infectors are assumed to uniformly mix in the crowd, which will cause deviation in the infection risk estimation for the close contact route. Thirdly, the hospital staff working in the waiting rooms are under much higher infection risk due to the prolonged exposure duration. Due to the lack of working schedule of the hospital staff, the assessment of infection risks of the staff has not been studied in this research. Another limitation of present study lies in the measurement of air change rate. Though CO_2 of steady state was considered to be less accurate as a tracer gas, it is the highly convenient and least disturbing method to obtain the air flow rate in enclosed space at the currant stage. Moreover, the air change rate of different locations in each space are different. As the air change rate in the breathing zone can better reflect the possibility of viral aerosol dilution and consequent COVID-19 infection risks, the indoor CO_2 measurement was only carried out in the breathing zone. This means the calculated air change rate may not represent the air flow rate of the entire space. Lastly, the patients flow during measurement was not taken into consideration. As Eq. (1) is only valid in the steady-state conditions and the present methodology tend to underestimate the air change rate with occupants number increasing between two consequent measurements and overestimate the air change rate with occupants number decreasing. In the future, this problem should be fixed by more frequent CO_2 concentration measurements or continuous online CO_2 monitoring.

From the perspective of transmission routes, COVID-19 is known to transmit through droplets, aerosols, and fomites. Though the droplet and aerosol transmission routes are reflected in the modified Wells-Riley model (Eq. (7)), the fomite transmission route is not covered in the present investigation. Moreover, the transmission of COVID-19 through indirect contact with virus aerosolized from patient's faces during flushing has also been brought forward, yet not included within the present investigation. Last but not least, the increased infection risk of doctors and nurses during medical operation procedures (such as the use of nebulizer on an infector) is also worth noticing and should be well-evaluated in the next stage of study.

7. Conclusions

A modified Wells-Riley model was introduced by combing airborne route and close contact route for the assessment of the infection probability of COVID-19 in an outpatient building in Shenzhen, China. The ventilation rates of the 20 waiting rooms, outpatient hall, and hospital street in the outpatient building were calculated by the occupant number and the difference between the on-site measured indoor and outdoor CO_2 concentration. The exposure duration was estimated by the number of patients and doctors on duty. This study provides a real-time monitoring method for the infection risk of COVID-19 in a closed space. Main findings include:

1) The average fresh air volume per person in the 20 waiting rooms was 77.6 m^3/h, 2 times of the Chinese standard. The average occupant area per person and exposure duration were 6.47 m^2/per and 0.69 h, respectively. Assuming an infector proportion of 2%, the daily average infection probability of COVID-19 for susceptible in the investigated outpatient building was 0.79% with a reasonable setting of $q = 45$ quanta/h and $\beta = 0.05$ h^{-1}. Assuming an infector proportion of 5%, 10% and 15% in the hospital for worse scenarios, the estimated daily average infection probabilities were 1.95%, 3.83%, and 5.64%, respectively.
2) The occupant areas per person in the waiting rooms of the ultrasound and anesthesiology department were the lowest among all of the waiting rooms, i.e., 2.6 m^2/per, and 3.1 m^2/per, accompanying with the lowest fresh air volume per person of 36.6 m^3/h and 39.7 m^3/h, which further resulted in the highest infection probability up to 1.88% and 1.44%, respectively, assuming an infector proportion of 2%. When all occupants in the waiting room wear medical surgical masks, the infection risks infection risks could be decreased by 75%.
3) With an occupant area per person of 8–20 m^2/per, a fresh air volume per person of 70–185 m^3/h and an exposure duration of 10 min, the estimated infection probability of COVID-19 in the hospital street, i.e., the main traffic space of the outpatient building was less than 0.04% assuming an infector proportion of 2% in the hospital street. The design of semi-closed hospital street improves the natural ventilation and thus reduces the infection risk of COVID-19.
4) Procedures should be taken to reduce the infection risks in the waiting rooms, including rising the air change rate or applying air cleaner to dilute/filter the viral aerosols, reduce the exposure duration by letting the patients waiting in the hospital street.

Author statement

The authors (Chunyin Li and Haida Tang) contributed equally to this work.

Declaration of competing interest

The authors declare that they have no known competing financial interests or personal relationships that could have appeared to influence the work reported in this paper.

Acknowledgments

The study described in this paper was supported by the National Natural Science Foundation of China (No. 52078296, 51808343, 52008254).

References

[1] Prashant Kumara, Lidia Morawska, Could fighting airborne transmission be the next line of defence against COVID-19 spread, City and Environment Interactions 4 (2019) 100033.
[2] Lidia Morawska, Donald K. Milton, It is time to address airborne transmission of COVID-19, Clin. Infect. Dis. 7 (2020), https://doi.org/10.1093/cid/ciaa939.
[3] J. Li, R. Gao, G. Wu, X. Wu, Z. Liu, H. Wang, Y. Huang, Z. Pan, J. Chen, X. Wu, Clinical Characteristics of Emergency Surgery Patients-Infected COVID-19 Pneumonia in Wuhan, 2020, https://doi.org/10.1016/j.surg.2020.05.007. China, Surgery.
[4] Chinese Center for Disease Control and Prevention, Epidemiological analysis of new coronavirus pneumonia, Chin. J. Epidemiol. 41 (2020) 145–151.
[5] Jianhui Peng, Liqi Xu, Mingke Wang, et al., Practical experiences on the prevention and treatment strategies to fight against COVID-19 in hospital, QJM: Int. J. Med. (2020) in press.
[6] A.L. Clarke, A.F. Stephens, S. Liao, et al., Coping with COVID-19: ventilator splitting with differential driving pressures using standard hospital equipment, Anaesthesia 75 (2020) 872–880.
[7] H. Qian, C. Zhang, X. Zheng, The function of aerosols in transmitting and infecting of respiratory infectious diseases and its risk prediction, Chin. Sci. Bull. 63 (2018) 931–939.
[8] C.M. Liao, Y.J. Lin, Y.H. Cheng, Modeling the impact of control measures on tuberculosis infection in senior care facilities, Build. Environ. 59 (2013) 66–75.
[9] H. Dai, B. Zhao, Association of the infection probability of COVID-19 with ventilation rates in confined spaces, Build. Simul. 13 (2020) 1321–1327.
[10] W.F. Wells, Airborne Contagion and Air Hygiene: an Ecological Study of Droplet Infection, Harvard University Press, Cambridge, MA, 1955.
[11] C. Fraser, S. Riley, R.M. Anderson, N.M. Ferguson, Factors that make an infectious disease outbreak controllable, Academy of Sciences of the United States of America 101 (2004) 6146–6151.
[12] R. Brookmeyer, E. Johnson, R Bollinger, Public health vaccination policies for containing an anthrax outbreak, Nature 432 (2004) 901–904.
[13] Y. Yan, X. Li, Y. Shang, et al., Evaluation of airborne disease infection risks in an airliner cabin using the Lagrangian-based Wells-Riley approach, Build. Environ. 121 (2017) 79–92.
[14] R. You, C.H. Lin, D. Wei, et al., Evaluating the commercial airliner cabin environment with different air distribution systems, Indoor Air 29 (2019) 840–853.
[15] H. Qian, Y. Li, P.V. Nielsen, et al., Spatial distribution of infection risk of SARS transmission in a hospital ward, Build. Environ. 44 (2009) 1651–1658.

[16] J. Hella, C. Morrow, F. Mhimbira, S. Ginsberg, N. Chitnis, S. Gagneux, et al., Tuberculosis transmission in public locations in Tanzania: a novel approach to studying airborne disease transmission, J. Infect. (2017) 191–197.
[17] S. Zhang, Z. Lin, Dilution-based evaluation of airborne infection risk-Thorough expansion of Wells-Riley model[J], Build. Environ. 194 (2021) 107674.
[18] C. Sun, Z. Zhai, The efficacy of social distance and ventilation effectiveness in preventing COVID-19 transmission[J], Sustainable cities and society 62 (2020) 102390.
[19] R. Sukarno, N. Putra, I.I. Hakim, et al., Utilizing heat pipe heat exchanger to reduce the energy consumption of airborne infection isolation hospital room HVAC system [J], Journal of Building Engineering 35 (2021) 102116.
[20] C. Chen, B. Zhao, Makeshift hospitals for COVID-19 patients: where health-care workers and patients need sufficient ventilation for more protection, J. Hosp. Infect. 105 (2020) 98–99.
[21] Shengwei Zhu, Jelena Srebric, John D. Spengler, Philip Demokritou, An advanced numerical model for the assessment of airborne transmission of influenza in bus microenvironments, Build. Environ. 47 (2012) 67–75.
[22] Mushayabasa Steady, Application of Wells–Riley equations on a mathematical model for assessing the transmission of tuberculosis in prison settings, International Journal of Modeling, Simulation, and Scientific Computing 4 (2013) 1350010.
[23] X. Gao, Y. Li, P. Xu, et al., Evaluation of intervention strategies in schools including ventilation for influenza transmission control, Building Simulation 5 (2012) 29–37.
[24] M. Zarrabi, S.A. Yazdanfar, S.B. Hosseini, COVID-19 and healthy home preferences: the case of apartment residents in Tehran[J], Journal of Building Engineering 35 (2021) 102021.
[25] Y. Wu, T.C.W. Tung, J.L. Niu, On-site measurement of tracer gas transmission between horizontal adjacent flats in residential building and cross-infection risk assessment, Build. Environ. 99 (2016) 13–21.
[26] Dick Menzies, Anne Fanning, Lilian Yuan, et al., Hospital ventilation and risk for tuberculous infection in Canadian health care workers, Ann. Intern. Med. 133 (2000) 779–789.
[27] P. Srikanth, S. Sudharsanam, R. Steinberg, Bio-aerosols in indoor environment: composition, health effects and analysis, Indian J. Med. Microbiol. 26 (2008) 302.
[28] R.E. Stockwell, E.L. Ballard, P. O'Rourke, et al., Indoor hospital air and the impact of ventilation on bioaerosols: a systematic review, J. Hosp. Infect. 103 (2019) 175–184.
[29] F.A. Berlanga, I. Olmedo, M. Ruiz de Adana, J.M. Villafruela, J.F. San José, F. Castro, Experimental assessment of different mixing air ventilation systems on ventilation performance and exposure to exhaled contaminants in hospital rooms, Energy Build. 177 (2018) 207–219.
[30] H. Qian, Y. Li, W.H. Seto, et al., Natural ventilation for reducing airborne infection in hospitals, Build. Environ. 45 (2010) 559–565.
[31] A. Agirman, Y.E. Cetin, M. Avci, et al., Effect of air exhaust location on surgical site particle distribution in an operating room, Build. Simul. 13 (2020) 979–988, https://doi.org/10.1007/s12273-020-0642-1.
[32] Y. Zhang, G. Cao, G. Feng, et al., The impact of air change rate on the air quality of surgical microenvironment in an operating room with mixing ventilation[J], Journal of Building Engineering 32 (2020) 101770.
[33] J. Wang, S. Wang, T. Zhang, F. Battaglia, Assessment of single-sided natural ventilation driven by buoyancy forces through variable window configurations, Energy Build. 139 (2017) 762–779.
[34] M. Cehlin, T. Karimipanah, U. Larsson, et al., Comparing thermal comfort and air quality performance of two active chilled beam systems in an open-plan office[J], Journal of Building Engineering 22 (2019) 56–65.
[35] G. Remion, B. Moujalled, M. El Mankibi, Review of tracer gas-based methods for the characterization of natural ventilation performance: comparative analysis of their accuracy, Build. Environ. 160 (2019) 106180.
[36] E. Zender–Świercz, Improvement of indoor air quality by way of using decentralised ventilation[J], Journal of Building Engineering 32 (2020) 101663.
[37] Haida Tang, Jianhua Ding, Chunying Li, Jiaxiong Li, A field study on indoor environment quality of Chinese inpatient buildings in a hot and humid region, Build. Environ. 151 (2019) 156~167.
[38] Jianxi Ma, Xiao Qi, Haoxuan Chen, et al., COVID-19 Patients in Earlier Stages Exhaled Millions of SARS-CoV-2 Per Hour, Clinical Infectious Diseases, 2020.
[39] N. Van Doremalen, T. Bushmaker, D.H. Morris, M.G. Holbrook, GambleA, et al., Aerosol and surface stability of SARS-CoV-2 as compared with SARS-CoV-1, N. Engl. J. Med. 382 (2020) 1564–1567.
[40] C.N. Haas, J.B. Rose, C.P. Gerba, Quantitative Microbial Risk, John Wiley & Sons, Inc., New York, 1999.
[41] X. Gao, J. Wei, B.J. Cowling, et al., Potential Impact of a Ventilation Intervention for Influenza in the Context of a Dense Indoor Contact Network in Hong Kong, Science of the Total Environment, 2016, pp. 373–381.
[42] D.S. Hui, B.K. Chow, L. Chu, S.S. Ng, N. Lee, et al., Exhaled air dispersion during coughing with and without wearing a surgical or N95 mask, PloS One 7 (2012), e50845.
[43] A. Davies, K.A. Thompson, K. Giri, G. Kafatos, J. Walker, A. Bennett, Testing the efficacy of homemade masks: would they protect in an influenza pandemic? Disaster Med. Public Health Prep. 7 (2013) 413–418.
[44] Ministry of Housing, Urban rural Development, Green Hospital Buildings Standard, 2015. GB/T 51153-2015.
[45] Ministry of Housing, Urban rural Development, Hygienic Standard for Hospital Waiting Room (GB 9671-1996), 1996.
[46] Taisheng Wang, Jing Lv, Dongdong Shi, Yiping Ma, Qihao Zhao, Research on personnel density and air conditioning cooling load in a general hospital, HV&AC. 45 (2015) 17–21 (in Chinese).
[47] Ministry of Housing, Urban rural Development, Code for Design of General Hospital (GB 51039-2014), 2014.
[48] G. Buonanno, L. Stabile, L. Morawska, Estimation of Airborne Viral Emission: Quanta Emission Rate of SARS-CoV-2 for Infection Risk Assessment, Environment International, 2020, p. 105794.
[49] Luo, Lei and Liu, Dan and Liao, Xin-long et al., Modes of Contact and Risk of Transmission in COVID-19: A Prospective Cohort Study 4950 Close Contact Persons in Guangzhou of China (3/29/2020). Available at: SSRN: https://ssrn.com/abstract=3566149 or https://doi.org/10.2139/ssrn.3566149.
[50] B. Blocken, T. van Druenen, A. Ricci, et al., Ventilation and air cleaning to limit aerosol particle concentrations in a gym during the COVID-19 pandemic[J], Build. Environ. 193 (2021) 107659.
[51] X. Zhang, Z. Ji, Y. Yue, et al., Infection risk assessment of COVID-19 through aerosol transmission: a case study of South China Seafood Market[J], Environ. Sci. Technol. 55 (7) (2021) 4123–4133.
[52] G. Buonanno, L. Morawska, L. Stabile, Quantitative assessment of the risk of airborne transmission of SARS-CoV-2 infection: prospective and retrospective applications[J], Environ. Int. 145 (2020) 106112.